

ARKANSAS POWER & LIGHT COMPANY

ARKANSAS NUCLEAR ONE

STEAM ELECTRIC STATION

UNIT TWO

CYCLE THREE

STARTUP REPORT

LICENSE NO. NPF-6

DOCKET NO. 50-368

FOR THE PERIOD ENDING JANUARY 4, 1983

WP-0676

8305230725 830512
PDR ADOCK 05000368
P PDR

TABLE OF CONTENTS

	PAGE
1.0 INTRODUCTION	1
2.0 PRECRITICAL TEST SUMMARIES	2
2.1 CEA Trip Test	2
2.2 Reactor Coolant Flow Coastdown	2
3.0 LOW POWER PHYSICS TEST SUMMARIES	3
3.1 Determination of Critical Boron Concentration	3
3.2 CEA Symmetry Test	3
3.3 Temperature Reactivity Coefficient	4
3.4 Part-Length Control Element Assembly (PLCEA) Reactivity Worth	7
3.5 Regulating CEA Group Reactivity Worth	7
3.6 Individual Control Element Assembly (CEA) 6-1 Reactivity Worth	9
3.7 Sequential Regulating Groups Reactivity Worth	9
4.0 POWER ESCALATION TEST SUMMARIES	9
4.1 Reactor Coolant Flow at 50% and 100% Full Power	9
4.2 Core Power Distribution at 50% and 100% Full Power	10
4.3 Shape Annealing Matrix (SAM) and Boundary Point Power Correlation (BPPC) Verification at 50% Full Power	23
4.4 Radial Peaking Factor and CEA Shadowing Factor Verification at 50% Full Power	25
4.5 Reactivity Coefficients at 50% and 100% Full Power	28
5.0 CONCLUSION	31

LIST OF TABLES AND FIGURES

	<u>PAGE</u>
Table 3.3-1 Isothermal Temperature Coefficient Measurement	6
Table 3.5-1 Regulating CEA Group Worths	8
Table 4.1-3 Reactor Coolant Flow at 50% and 100% Full Power	11
Table 4.2-1 Core Power Distribution at 50% Full Power	13
Table 4.2-2 Core Power Distribution at 100% Full Power	18
Table 4.3-1 Shape Annealing Matrix (SAM) and Boundary Point Power Correlation Coefficients	24
Table 4.4-1 Radial Peaking Factors	26
Table 4.4-2 CEA Shadowing Factors	27
Table 4.5-1 Reactivity Coefficients at 50% and 100% Full Power	30
Figure 4.2-1 (a) - 4.2-1 (d) Radial Power Distribution at 50% Full Power	14-17
Figure 4.2-2 (a) - 4.2-2 (d) Radial Power Distribution at 100% Full Power	19-22

1.0 INTRODUCTION

Post fuel load startup testing of Arkansas Nuclear One, Unit 2 commenced November 8, 1982 with the performance of precritical tests. Low power physics testing began on November 10, 1982. On this date at 0744 Cycle 3 initial criticality was achieved. Low power physics testing proceeded to completion at 1900 on November 13, 1982 at which time power ascension testing commenced. The first power ascension test plateau (50% full power) was attained on November 25, 1982. Following completion of testing at 50% full power on December 16, 1982, reactor power was raised to 100% full power and testing continued. The power escalation test program was completed on January 4, 1983.

2.0 PRECRITICAL TEST SUMMARIES

2.1 CEA Trip Test

2.1.1 Purpose

The CEA trip test was performed to verify that the elapsed time between initiation of a CEA trip and 90% insertion of the CEA was ≤ 3.0 seconds.

2.1.2 Test Method

Initial reactor coolant system conditions were established with $T_{avg} \geq 525^{\circ}\text{F}$ and four reactor coolant pumps operating. One CEA group was then fully withdrawn. As each CEA in that group was dropped (by removing electrical power from the drive mechanism), the elapsed time between initiation of the trip and 90% insertion of the CEA was recorded. After completing drop time testing on one CEA group, the next CEA group was tested. Drop time testing proceeded in this manner until all designated CEAs had been tested.

2.1.3 Results and Evaluation

The measured individual full length CEA drop times from a fully withdrawn position to 90% insertion were < 3.0 seconds.

2.2 Reactor Coolant Flow Coastdown

2.2.1 Purpose

The reactor coolant flow coastdown test was performed to verify the response time of Channel C core protection calculator to a two out of four reactor coolant pump trip and flow coastdown.

2.2.2 Test Method

Initial reactor coolant system conditions were established with four reactor coolant pumps running. Recording instrumentation was connected to the status contacts of two separate-loop RCP motor power supply breakers and CEDM coil monitors. With appropriate test software loaded in CPC Channel C, the two reactor coolant pumps were tripped simultaneously. The elapsed time between initiation of the pump trip and receipt of a low DNBR trip from the core protection calculator was measured.

2.2.3 Results and Evaluation

The measured response time of CPC Channel C to a two-pump loss of flow transient was 0.295 seconds. The maximum acceptable response time is 0.80 seconds.

3.0 LOW POWER PHYSICS TEST SUMMARIES

3.1 Determination of Critical Boron Concentration

3.1.1 Purpose

The reactor coolant system boron concentration required to maintain criticality of the reactor at the beginning of Cycle 3 under hot zero power xenon-free conditions was measured. The results of this measurement were compared to predictions to verify design, fabrication and proper loading of the core.

3.1.2 Test Method

Criticality of the reactor was obtained by deboration of the reactor coolant system at a constant dilution rate. All CEAs were fully withdrawn prior to deborating the RCS with the exception of regulating group 6 which was 75" withdrawn. Once criticality was achieved, the dilution was terminated and the RCS boron concentration allowed to equilibrate. The critical boron concentration was calculated by correcting the measured equilibrium boron concentration for deviation of CEA position from the reference (ARO) CEA position and compared to the predicted critical ARO boron concentration.

3.1.3 Results and Evaluation

The measured critical boron concentration of 1272 ppm agreed well with the predicted value of 1275. Acceptance criteria state that the measured critical boron concentration shall be within 100 ppm of the predicted critical boron concentration.

3.2 CEA Symmetry Test

3.2.1 Purpose

A CEA symmetry test was performed to verify that all CEAs were coupled to their extension shafts and to verify correct loading of the core.

3.2.2 Test Method

The symmetry checks were performed by inserting the reference CEA of a group to its lower electrical limit and compensating for the reactivity change by withdrawing CEA regulating group 6. Symmetric CEAs in the group were subsequently traded with each other and the reactivity deviation from the reference CEA measured. The reference CEA was finally traded for the last symmetric CEA in the group to measure reactivity drift. The adjusted deviation was calculated by adding the appropriate drift correction to the CEA worth deviation from the reference CEA. CEA coupling was verified by noting a change in reactivity when a CEA was inserted.

3.2.3 Results and Evaluation

The absolute value of adjusted reactivity deviation for all CEAs from their respective references was less than the maximum acceptable value of 1.5 cents. All CEAs were verified to be coupled.

3.3 Temperature Reactivity Coefficient

3.3.1 Purpose

The isothermal temperature coefficient (ITC) measurement was performed during low power physics testing to verify conformance with Technical Specifications on the moderator temperature coefficient (MTC). Comparison of the measured ITC to predictions was also performed to demonstrate proper design and fabrication of the core.

3.3.2 Test Method

The isothermal temperature coefficient was measured at two CEA configurations: essentially all rods out (CEA group 6 > 130" withdrawn) and the zero power insertion limit.

At the specified CEA configuration, the test was initiated by decreasing average reactor coolant temperature by approximately 10°F and then increasing the temperature to its initial value. During the change in temperature, reactivity feedback was compensated for by CEA regulating group movement. This compensation was required to maintain reactor power within the acceptable test range. The reactivity change associated with the change in RCS average temperature was obtained from the reactivity computer and used to calculate the ITC.

After the ITC had been measured, a predicted value of the fuel temperature coefficient was subtracted from the ITC to obtain the MTC.

3.3.3 Results and Evaluation

Table 3.3-1 tabulates the results of the temperature reactivity coefficient measurement. All applicable acceptance criteria were met.

TABLE 3.3-1

ISOTHERMAL TEMPERATURE COEFFICIENT MEASUREMENT

		MEASURED ($\times 10^{-4} \Delta k/k/^{\circ}F$)	PREDICTED ($\times 10^{-4} \Delta k/k/^{\circ}F$)	ACCEPTANCE CRITERIA
1. ARO	ITC	-0.01	-0.01	(a)
	MTC	+0.15	+0.15	(b)
2. ZPIL	ITC	-0.13	-0.1	(a)
	MTC	+0.03	+0.05	(b)

NOTES:

- (a) Measured value must be within $\pm 0.3 \times 10^{-4} \Delta k/k/^{\circ}F$ of predicted value.
- (b) Measured value must be less positive than $+ 0.5 \times 10^{-4} \Delta k/k/^{\circ}F$.

3.4 Part-Length Control Element Assembly (PLCEA) Reactivity Worth

3.4.1 Purpose

This test was performed for information only. The results will be utilized in reactivity balance calculations.

3.4.2 Test Method

PLCEA group reactivity worth to 75" withdrawn was measured at hot zero power conditions using the boron/PLCEA swap method. This method consists of establishing a constant deboration rate in the RCS and compensating for the reactivity change by inserting the PLCEAs in incremental steps. This process was reversed to obtain the withdrawal measurement of PLCEA reactivity worth.

The reactivity change values that occurred during these measurements were obtained from the reactivity computer and were correlated with PLCEA group position.

3.4.3 Results and Evaluation

This measurement was made for information only. Hence, no quantitative acceptance criteria were applied.

3.5 Regulating CEA Group Reactivity Worth

3.5.1 Purpose

The reactivity worths of the CEA regulating groups were measured to verify calculations of available shutdown margin. The results of this test were compared to vendor predictions of regulating group reactivity worth. If sufficient agreement between prediction and measurement is demonstrated for the regulating CEA group reactivity worths, the reactivity worth predictions for the shutdown CEA groups are deemed adequate. Additionally, the measured values of regulating CEA reactivity worth can be utilized for reactivity balance calculations.

3.5.2 Test Method

The regulating group reactivity worths were measured at hot zero power conditions using the boron/CEA group swap method. Reference section 3.4.2 for the test method.

3.5.3 Results and Evaluation

Table 3.5-1 tabulates the results of the regulating CEA group reactivity worth measurement. All applicable acceptance criteria were met.

TABLE 3.5-1			
REGULATING CEA GROUP WORTHS			
REGULATING GROUP NUMBER	MEASURED WORTH (% Δ k/k)	PREDICTED WORTH (% Δ k/k)	ACCEPTANCE CRITERIA (% Δ k/k)
6	0.51	0.56	± 0.10
5	0.47	0.54	± 0.10
4	0.47	0.43	± 0.10
3	0.85	0.95	± 0.14
2	0.61	0.63	± 0.10
1	1.08	1.14	± 0.17
TOTAL	3.99	4.25	± 0.42

3.6 Individual Control Element Assembly (CEA) 6-1 Reactivity Worth

3.6.1 Purpose

This test was performed for information only. The results were utilized in the 50% power ITC/MTC measurement.

3.6.2 Test Method

CEA 6-1 reactivity worth was measured at hot zero power using the reactivity computer. Reactivity changes were measured and correlated with CEA 6-1 positions during both insertion and withdrawal of CEA 6-1.

3.6.3 Results and Evaluation

This measurement was made for information only. Hence, no quantitative acceptance criteria were applied.

3.7 Sequential Regulating Groups Reactivity Worth

3.7.1 Purpose

This test was performed for information only.

3.7.2 Test Method

Sequential reactivity worth was measured at hot zero power from the zero power dependent insertion limit to all rods out. A constant boration rate was maintained to group 6 at approximately 130" withdrawn and then an incremental pull made to determine worth of group 6 from 130" to all rods out.

3.7.3 Results and Evaluation

This measurement was made for information only. Hence, no quantitative acceptance criteria were applied.

4.0 POWER ESCALATION TEST SUMMARIES

4.1 Reactor Coolant Flow at 50% and 100% Full Power

4.1.1 Purpose

Measurement of reactor coolant flow was carried out at 50% and 100% full power utilizing calorimetric methods. The results were used to verify the conservatism of the Core Operating Limit Supervisory System (COLSS) and the Core Protection Calculator (CPC) measurements of reactor coolant flow.

4.1.2 Test Method

A calorimetric measurement of reactor coolant flow was performed at steady state conditions. After establishing initial conditions for test performance, reactor core ΔT , primary system pressure, and secondary calorimetric power were recorded. From these state parameters, RCS mass flow was computed from the following:

$$m = Q/\Delta h$$

where

Q = Secondary calorimetric power (BTU/hr)

$\Delta h = h_H - h_C$ = difference between hot leg and cold leg
specific enthalpy (BTU/lb_m)

m = RCS mass flowrate (lb_m/hr)

The calorimetric RCS mass flow was then compared to COLSS RCS mass flow and appropriate adjustments to COLSS flow constants were made. CPC RCS mass flow was next compared to COLSS RCS mass flow. Adjustments to the appropriate CPC constants were made to maintain the CPC value of RCS flow conservative with respect to the COLSS value of RCS flow.

4.1.3 Results and Evaluation

Acceptance criteria applied to this test at 50% and 100% full power state that for COLSS operable, measured RCS flow must be greater than COLSS calculated RCS flow which in turn must be greater than CPC calculated RCS flow. Table 4.1-1 summarizes the results of this test. Applicable acceptance criteria were met at 50% and 100% full power.

TABLE 4.1-3

REACTOR COOLANT FLOW At 50% AND 100% FULL POWER

TEST PLATEAU (PERCENT FULL POWER)	MEASURED FLOW ⁽¹⁾	COLSS FLOW ⁽¹⁾	CPC FLOW ⁽¹⁾			
			A	B	C	D
50%	107.86	106.02	101.86	101.78	101.66	101.52
100%	113.57	113.38	113.15	113.12	113.13	113.16

⁽¹⁾ Flow values reported in percent of design mass flow.

4.2 Core Power Distribution at 50% and 100% Full Power

4.2.1 Purpose

Steady state core power distribution was measured at 50% and 100% full power to verify core nuclear and thermal-hydraulic calculational models, thereby justifying use of these models for performing the cycle 3 safety analysis. This test also serves to verify acceptable operating conditions at each test plateau.

4.2.2 Test Method

Steady state reactor power was established at the appropriate test plateau with equilibrium xenon. Incore detector data was then collected and analyzed using an incore analysis computer code. Specified power distribution parameters were obtained from the code and compared to predictions to verify the acceptability of the measured power distribution.

4.2.3 Results and Evaluation

Tables 4.2-1 and 4.2-2 tabulate the results of the core power distribution tests. Figures 4.2-1 and 4.2-2 depict the measured radial power distributions at 50% and 100% full power. All applicable acceptance criteria for this test were met.

Deviation of predicted versus measured radial relative power density did not meet the requirements of the additional review criteria (see note 6 of Table 4.2-1) for all fuel assemblies. Evaluation by the Nuclear Engineering section of Arkansas Power & Light and Combustion Engineering was performed and presented to the Plant Safety Committee. The PSC concurred that all acceptance criteria were met and that the minor deviations from predicted relative power densities did not constitute a safety concern.

TABLE 4.2-1

CORE POWER DISTRIBUTION AT 50% FULL POWER

PARAMETER	MEASURED	PREDICTED	DIFFERENCE	ACCEPTANCE CRITERIA ⁽⁶⁾
RMS ⁽¹⁾ (axial)	4.9422	--	--	≤ 5.000
RMS ⁽¹⁾ (radial)	4.9997	--	--	≤ 5.000
F _{xy} ⁽²⁾	1.4880	1.50	-.008	± 0.16
F _r ⁽³⁾	1.4683	1.45	+.0126	± 0.16
F _z ⁽⁴⁾	1.2858	1.22	+.0539	± 0.12
F _Q ⁽⁵⁾	1.9050	1.75	+.0886	± 0.19

$$(1) \text{ RMS} = \left[\sum_{i=m}^n (100h_i)^2 / n \right]^{1/2}$$

where h_i = difference between the predicted and measured relative power density for the i^{th} axial or radial node.

$m, n = 1, 101$ for the axial distribution

$m, n = 1, 177$ for the radial distribution

(2) F_{xy} = Planar radial peaking factor

(3) F_r = Integrated planar radial peaking factor

(4) F_z = Core average axial peaking factor

(5) F_Q = Three dimensional power peaking factor

(6) Additional review criteria requires that for each assembly with a predicted relative power density ≥ 0.9 , the measured relative power density (RPD) must agree with the predicted RPD to within $\pm 10\%$ of the predicted value. For each assembly with a predicted RPD < 0.9 , the measured RPD must agree with the predicted RPD to within $\pm 15\%$ of the predicted value.

FIGURE 4.2-1 (a)

RADIAL POWER DISTRIBUTION AT 50% FULL POWER

	A	B	C	D	E	F	G
1						.729 .691 5.50	1.01 .945 6.90
2				.768 .725 6.10	1.04 .977 6.46	.919 .882 4.17	1.18 1.12 5.38
3			.853 .805 5.96	1.12 1.06 5.63	1.03 .998 3.22	1.26 1.232 2.31	.981 .983 .39
4		.768 .728 5.48	1.11 1.050 5.71	1.17 1.123 4.21	1.29 1.255 2.76	.916 .933 -1.84	1.22 1.245 -1.99
5		1.04 .996 4.38	1.03 1.003 2.72	1.29 1.267 1.78	.922 .946 -2.51	.985 1.033 -4.61	.871 .939 -7.23
6	.727 .692 5.07	.917 .898 2.13	1.26 1.23 2.10	.915 .934 -2.01	.985 1.029 -4.30	1.09 1.166 -6.53	.815 .926 -12.00
7	1.01 .968 4.38	1.17 1.171 -.06	.984 .989 -.48	1.22 1.240 -1.59	.870 .931 -6.52	.818 .904 -9.51	1.04 1.159 -10.24

x.xxx	Predicted
y.yyy	Measured
z.zzz	Percent Difference

NW

FIGURE 4.2-1 (b)

RADIAL POWER DISTRIBUTION AT 50% FULL POWER

H	J	K	L	M	N	P	R	
1.05	1.01	.727						1
.987	.955	.699						
6.44	5.77	4.07						
.946	1.17	.917	1.04	.768				2
.921	1.142	.892	.983	.734				
2.74	2.48	2.78	5.80	4.58				
1.02	.984	1.26	1.03	1.11	.853			3
1.023	.989	1.243	1.011	1.081	.828			
-.33	-.52	1.38	1.86	2.66	3.02			
.921	1.22	.915	1.29	1.17	1.12	.769		4
.960	1.239	.939	1.279	1.150	1.089	.751		
-4.08	-1.53	-2.60	.87	1.70	2.84	2.44		
1.06	.870	.985	.922	1.29	1.03	1.04		5
1.126	.937	1.038	.961	1.298	1.035	1.021		
-5.89	-7.14	-5.10	-4.05	-.65	-.45	1.87		
.911	.818	1.09	.985	.916	1.26	.919	.729	6
1.009	.918	1.168	1.044	.955	1.285	.908	.703	
-9.71	-10.90	-6.65	-5.61	-4.06	-1.97	1.26	3.67	
.910	1.04	.815	.871	1.22	.987	1.18	1.01	7
.918	1.144	.897	.929	1.248	.995	1.13	.952	
-11.76	-9.07	-9.10	-6.27	-2.22	-.82	4.40	6.12	

x.xxx	Predicted
y.yyy	Measured
z.zzz	Percent Difference

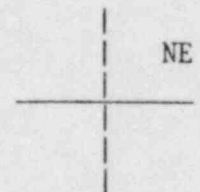


FIGURE 4.2-1 (c)

RADIAL POWER DISTRIBUTION AT 50% FULL POWER

8	1.05	.946	1.02	.921	1.06	.911	.810
	1.002	.931	1.001	.951	1.119	1.001	.938
	4.02	1.60	1.89	-3.19	-5.29	-9.00	-13.63
9	1.01	1.16	.981	1.22	.871	.815	1.04
	.965	1.144	.987	1.233	.917	.895	1.154
	4.66	2.73	-.03	-1.014	-5.06	-8.95	-9.86
10	.729	.919	1.26	.916	.985	1.09	.818
	.706	.903	1.256	.927	.984	1.141	.923
	3.20	1.81	.29	-1.13	.09	-4.48	-11.40
11		1.04	1.03	1.29	.922	.985	.870
		1.006	1.012	1.256	.916	1.009	.927
		3.33	1.75	2.72	.68	-2.37	-6.10
12		.769	1.12	1.17	1.24	.915	1.22
		.740	1.073	1.109	1.195	.909	1.225
		3.93	4.35	5.51	7.96	.63	-.39
13			.853	1.11	1.03	1.26	.984
			.811	1.052	.981	1.213	.974
			5.19	5.49	5.03	3.86	1.06
14				7.68	1.04	.917	1.17
				7.26	.988	.880	1.121
				5.63	5.32	4.21	4.41
15						.727	1.01
						.681	.943
						5.45	7.13

A

B

C

D

E

F

G

x.xxx	Predicted
y.yyy	Measured
z.zzz	Percent Difference

SW

FIGURE 4.2-1 (d)

RADIAL POWER DISTRIBUTION AT 50% FULL POWER

.584	.810	.911	1.06	.921	1.02	.946	1.05	8
.673	.906	.982	1.098	.949	1.011	.917	.984	
-13.25	-10.57	-7.21	-3.43	-2.99	.93	3.22	6.66	
.810	1.04	.818	.870	1.22	.984	1.17	1.01	9
.913	1.136	.883	.907	1.226	.982	1.127	.946	
-11.28	-8.42	-7.40	-4.07	-.46	.20	3.60	6.74	
.911	.815	1.09	.985	.915	1.26	.917	.727	10
1.002	.910	1.134	.976	.923	1.250	.892	.690	
-9.08	-10.47	-3.91	.92	-.89	.77	2.80	5.42	
1.06	.871	.985	.922	1.29	1.03	1.04	11	
1.116	.927	1.016	.931	1.264	1.010	1.000		
-4.98	-6.06	-3.06	-.95	2.08	1.98	4.05		
.921	1.22	.916	1.29	1.17	1.11	.768	12	
.951	1.234	.929	1.258	1.128	1.068	.735		
-3.16	-1.12	-1.36	2.52	3.74	3.98	4.46		
1.02	.987	1.26	1.03	1.12	.853	13		
1.015	.982	1.231	1.001	1.066	.814			
.493	.56	2.33	2.92	5.12	4.86			
.946	1.18	.919	1.04	.769	14			
.916	1.130	.887	.983	.729				
3.33	4.39	3.67	5.83	5.55				
1.05	1.01	.729	15					
.981	.948	.694						
7.00	6.59	5.10						

H J K L M N P R

x.xxx	Predicted
y.yyy	Measured
z.zzz	Percent Difference

	SE

TABLE 4.2-2

CORE POWER DISTRIBUTION AT 100% FULL POWER

PARAMETER	MEASURED	PREDICTED	DIFFERENCE	ACCEPTANCE CRITERIA ⁽⁶⁾
RMS ⁽¹⁾ (axial)	2.85	--	--	≤ 5.000
RMS ⁽¹⁾ (radial)	4.25	--	--	≤ 5.000
F _{xy} ⁽²⁾	1.49	1.47	+ .0136	$\pm .15$
F _r ⁽³⁾	1.47	1.45	+ .0138	$\pm .14$
F _z ⁽⁴⁾	1.18	1.19	- .0084	$\pm .12$
F _Q ⁽⁵⁾	1.76	1.71	+ .0292	$\pm .17$

Note: Superscripts refer to footnotes of Table 4.2-1

FIGURE 4.2-2 (a)

RADIAL POWER DISTRIBUTION AT 100% FULL POWER

	A	B	C	D	E	F	G
1						.677 .704 -3.89	.923 .957 3.58
2				.707 .740 -4.49	.945 1.00 -5.47	.862 .897 -3.96	1.09 1.14 -4.46
3			.787 .819 -3.90	1.04 1.07 -3.09	.977 1.01 -3.28	1.21 1.24 2.14	.975 .989 -1.44
4		.714 .74 -3.54	1.02 1.07 -4.52	1.10 1.13 -2.44	1.23 1.27 -2.795	.934 .935 -1.107	1.26 1.24 1.92
5		.980 1.00 -1.97	.987 1.01 -2.31	1.26 1.27 -1.02	.952 .944 .805	1.05 1.02 3.19	.964 .921 4.70
6	.680 .703 -3.26	.882 .896 -1.55	1.22 1.24 -1.74	.941 .934 .760	1.07 1.02 4.58	1.21 1.14 6.21	.978 .879 11.26
7	.950 .956 .638	1.141 1.140 .105	.989 .987 .187	1.26 1.24 1.68	.960 .920 4.38	.945 .882 7.17	1.23 1.12 10.09

x.xxx	Predicted
y.yyy	Measured
z.zzz	Percent Difference

NW

FIGURE 4.2-2 (b)

RADIAL POWER DISTRIBUTION AT 100% FULL POWER

H	J	K	L	M	N	P	R	
.963 .993 -3.00	.930 .956 -2.72	.682 .703 -3.04						1
.900 .926 -2.85	1.11 1.14 -3.00	.867 .896 -3.23	.945 1.00 -5.49	.713 .740 -3.68				2
1.02 1.03 -1.46	.977 .987 -1.03	1.22 1.24 -1.74	.985 1.01 -2.50	1.05 1.07 -1.50	.81 .819 -1.06			3
.971 .954 1.75	1.25 1.24 .879	.934 .934 .0428	1.25 1.27 -1.57	1.13 1.13 -0.389	1.06 1.07 -0.495	.736 .740 -0.595		4
1.16 1.11 4.20	.957 .920 4.00	1.05 1.02 2.48	.958 .944 1.50	1.28 1.27 .583	1.011 1.01 .109	.998 1.00 -0.21		5
1.06 .98 7.82	.96 .882 8.89	1.20 1.14 5.27	1.07 1.02 4.53	.950 .935 1.57	1.25 1.24 .653	.882 .897 -1.68	.685 .704 -2.70	6
.971 .890 9.15	1.21 1.12 8.11	.93 .879 5.84	.950 .921 3.14	1.25 1.24 .984	.979 .989 -0.991	1.09 1.14 -4.32	.924 .957 -3.41	7

x.xxx	Predicted
y.yyy	Measured
z.zzz	Percent Difference

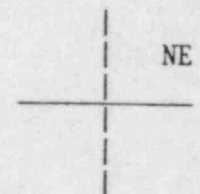


FIGURE 4.2-2 (c)

RADIAL POWER DISTRIBUTION AT 100% FULL POWER

8	.9879 .9930 -.514	.922 .926 -.410	1.028 1.03 -.214	.973 .954 2.03	1.16 1.11 4.44	1.05 .980 7.58	1.01 .890 13.82
9	.950 .957 -.700	1.125 1.14 -1.32	.990 .989 .071	1.26 1.24 1.23	.948 .921 2.93	.938 .879 6.70	1.23 1.12 9.83
10	.698 .704 -.909	.889 .897 -.870	1.244 1.24 .323	.936 .935 .096	1.023 1.02 .284	1.19 1.14 4.34	.980 .882 11.10
11		.989 1.00 -1.12	.996 1.01 -1.44	1.25 1.27 -1.64	.929 .944 -1.61	1.03 1.02 1.39	.954 .92 3.71
12		.721 .740 -2.55	1.03 1.07 3.36	1.09 1.13 -3.27	1.20 1.27 -5.82	.918 .934 -1.70	1.242 1.240 .145
13			.790 .819 -3.50	1.03 1.07 -3.42	.97 1.01 -3.96	1.21 1.24 -2.63	.975 .987 -1.25
14				.711 .740 -3.86	.962 1.00 -3.80	.871 .896 -2.79	1.11 1.14 -2.35
15						.686 .703 -2.46	.937 .956 -1.95

A	B	C	D	E	F	G
x.xxx	Predicted					
y.yyy	Measured					
z.zzz	Percent Difference					

SW

FIGURE 4.2-2 (d)

RADIAL POWER DISTRIBUTION AT 100% FULL POWER

.7230	.975	1.03	1.13	.959	1.01	.894	.958	8
.656	.890	.980	1.11	.954	1.03	.926	.993	
-10.20	-9.53	4.94	2.21	.503	-2.06	-3.43	-3.50	
.967	1.20	.917	.930	1.23	.970	1.09	.919	9
.890	1.12	.682	.920	1.24	.987	1.14	.956	
8.60	7.20	4.01	1.03	-.565	-1.80	-4.29	-3.85	
1.05	.947	1.17	1.01	.922	1.22	.868	.670	10
.980	.879	1.14	1.02	.934	1.24	.896	.703	
7.07	7.68	2.43	-1.44	-1.28	-1.49	-3.13	-4.77	
1.15	.946	1.03	.933	1.25	.986	.975		11
1.11	.921	1.02	.944	1.27	1.01	1.00		
3.26	2.71	.941	-1.22	-1.95	-2.43	-2.53		
.963	1.243	.927	1.24	1.10	1.03	.715		12
.954	1.24	.935	1.27	1.13	1.07	.74		
.902	.226	-.834	-2.36	-2.37	-3.74	-3.42		
1.02	.976	1.21	.980	1.04	.791			13
1.03	.989	1.24	1.01	1.07	.819			
-1.46	-1.29	-2.02	-2.97	-2.87	-3.42			
.909	1.11	.871	.951	.710				14
.926	1.14	.897	1.00	.740				
-1.87	-2.38	-2.95	-4.94	-4.12				
.974	.937	.686						15
.993	.957	.704						
-1.92	-2.07	-2.63						

H

J

K

L

M

N

P

R

x.xxx

y.yyy

z.zzz

Predicted

Measured

Percent Difference

SE

4.3 Shape Annealing Matrix (SAM) and Boundary Point Power Correlation (BPPC) Verification at 50% Full Power

4.3.1 Purpose

Measurement of the SAM elements and BPPC constants was performed to determine acceptable values of these constants for a wide range of core axial power shapes.

4.3.2 Test Method

The SAM elements and BPPC constants were determined from a least squares analysis of the measured excore detector readings and the corresponding power distribution determined from the incore detector signals. Since these values must be representative of the range of axial power distributions expected throughout cycle 3, it was desirable to measure these parameters within the expected range of axial shapes. This was done by initiating an axial xenon oscillation and periodically recording incore, excore and reactor state parameters during the oscillation. The incore data was analyzed using an incore analysis computer code to obtain third core peripheral power integrals, third core detector fractional response, upper and lower third core integrals of core average power and upper and lower core boundary point powers. A least squares analysis was then performed to obtain the optimum set of SAM elements and BPPC constants characterizing the correlation between the excore detectors measured response and the corresponding incore detectors power distributions. The analysis was performed for each CPC channel.

4.3.3 Results and Evaluation

Acceptance criteria for this test required that new SAM values be installed in each CPC. An identical acceptance criteria required new BPPC coefficients to be installed in each CPC also.

For each SAM calculated, a test value characterizing the "goodness of fit" of each matrix was computed. Acceptable test values were obtained for each matrix. Hence, no further adjustments to the CPCs were necessary. Table 4.3-1 tabulates the results of the test.

TABLE 4.3-1
SHAPE ANNEALING MATRIX (SAM) AND
BOUNDARY POINT POWER CORRELATION COEFFICIENTS

CPC CONSTANT	PID	MEASURED VALUE			
		CHANNEL A	CHANNEL B	CHANNEL C	CHANNEL D
SC11	81	6.6590	8.0331	7.4801	8.1628
SC12	82	-0.34392	-2.7589	-2.2663	-3.6006
SC13	83	-3.34951	-2.0730	-2.0708	-1.2090
SC21	84	-0.79157	-2.2349	-2.3979	-2.3527
SC22	85	4.1830	6.9794	7.1580	7.0390
SC23	86	-0.10430	-1.7922	-1.7992	-1.7236
SC31	87	-2.8675	-2.7982	-2.0823	-2.8101
SC32	88	-0.83909	-1.2205	-1.8917	-0.4384
SC33	89	6.4538	6.8651	6.8700	5.9326
BPPCC1	99	0.80603 E-2	0.80589 E-2	0.80601 E-2	0.80589 E-2
BPPCC2	100	0.30067 E-1	0.30039 E-1	0.30061 E-1	0.30039 E-1
BPPCC3	101	0.89769 E-2	0.89812 E-2	0.89773 E-2	0.89774 E-2
BPPCC4	102	0.42395 E-1	0.42537 E-1	0.42405 E-1	0.42415 E-1
(1) Test Value	---	4.3675	4.7597	4.7431	4.7006

(1) No further CPC adjustments required if test value ≤ 6.1313 .

4.4 Radial Peaking Factor and CEA Shadowing Factor Verification at 50% Full Power

4.4.1 Purpose

Performance of this test at 50% full power assured conservatism of the radial peaking factors (RPFs) utilized by the CPCs and COLSS in the power distribution synthesis algorithms. In addition, the adequacy of the predicted CEA shadowing factors (CSFs) installed in the CPCs was demonstrated.

4.4.2 The performance of this test involved establishing the following CEA configurations:

All CEAs out

Group 6 at LEL (Lower Electrical Limit)

Group 6 at LEL, Group 5 at LEL withdrawn

Group 6 at LEL, Group 5 at LEL, Group P at 37.5" wd.

Group 6 at LEL, Group P at 37.5" wd.

Group P at 37.5" wd.

At each CEA configuration, incore and excore data were recorded. This data was analyzed to determine the planar radial peaking factors and CEA shadowing factors for the particular CEA configuration. Appropriate corrections were applied to the RPF and CSF multipliers (ARM, $i = 1$ to 6; ASM, $i = 2$ to 7) to guarantee conservatism of the applied RPFs and to assure the adequacy of the applied CSFs.

4.4.3 Results and Evaluations

Tables 4.4-1 and 4.4-2 summarize the results of the radial peaking factor and CEA shadowing factor test. All necessary adjustments to appropriate CPC and COLSS constants were made based upon measured RPFs and CSFs.

TABLE 4.4-1		
RADIAL PEAKING FACTORS		
CEA GROUP/POSITION	F _{xy}	
	MEASURED	PREDICTED
ARO	1.4790	1.50
6/LEL	1.6188	1.70
6/LEL, 5/LEL	1.6695	1.61
6/LEL, 5/LEL, P/37.5"	1.6722	1.56
6/LEL, P/37.5"	1.6625	1.78
P/37.5"	1.4985	1.57

TABLE 4.4-2
CEA SHADOWING FACTORS

CEA GROUP/POSITION	PREDICTED CSF	MEASURED CSF			
		CHANNEL A	CHANNEL B	CHANNEL C	CHANNEL D
6/LEL	1.05	.99933	1.00209	1.00604	.99139
6/LEL, 5/LEL	0.92	.92395	.92215	.91615	.91752
6/LEL, 5/LEL, P/37.5"	0.98	.90897	.90681	.89953	.89953
6/LEL, P/37.5"	1.11	1.04180	1.04573	1.04755	1.0305
P/37.5"	1.05	N/A	N/A	N/A	N/A

4.5 Reactivity Coefficients at 50% and 100% Full Power

4.5.1 Purpose

Temperature reactivity coefficients were measured at 50% and 100% full power to verify that these parameters were within the range specified in Technical Specifications. A power reactivity coefficient measurement was performed in conjunction with the temperature reactivity coefficient measurement at 50% full power. In addition to verifying compliance with Technical Specifications, these measurements aid in verifying proper design and fabrication of the reload core and provide an expanded data base for reactivity balance calculations.

4.5.2 Test Method

Two methods were used to determine the isothermal temperature coefficient (ITC) and power coefficient (PC); one method relies upon center CEA movement while the other method does not utilize movement of the center CEA.

4.5.2.1 Reactivity Coefficient Measurement with Center CEA Movement at 50% Full Power

Measurement of the isothermal temperature coefficient (ITC) and power coefficient (PC) using center CEA movement was performed in two stages. Initial conditions were established with the reactor at steady state, equilibrium xenon and CEA group 6 at 120 inches withdrawn. The ITC portion of the test was started by initiating a small increase in turbine load. Reactor power was held essentially constant by insertion of the center CEA while reactor coolant temperature was allowed to decrease. After the system had stabilized at the new steady state conditions, data was collected and the process described above reversed. This sequence was repeated to assure data was consistent and to reduce experimental uncertainty. Following completion of this phase of the test, initial conditions were re-established for the PC portion of the test. This phase of the measurement was initiated by decreasing turbine load while withdrawing the center CEA to maintain reactor coolant temperature constant. Reactor power was allowed to increase and stabilize at a new steady state. This process was reversed following a short data collection period at the new steady state. The entire cycle was then repeated to

assure data was consistent and to reduce experimental uncertainty. Data obtained from the test was reduced to obtain two equations in which the ITC and PC were independent variables. These equations were solved simultaneously utilizing an iterative solution technique to obtain the ITC and PC. The moderator temperature coefficient (MTC) was calculated by subtracting the predicted fuel temperature coefficient from the measured ITC.

4.5.2.2 Temperature Reactivity Coefficient Measurement without Center CEA Movement at 100% Full Power

With the reactor at steady state, equilibrium xenon and CEA group 6 at 120 inches withdrawn, a small step change in the turbine control valve position was made and then adjusted to establish a new coolant inlet temperature. This change produced a small turbine load-reactor power mismatch. The temperature change resulted in a reactivity feedback and a resultant power change. The power change produced an opposite reactivity feedback and the reactor settled out at a new power and temperature condition. The cycle was then reversed by making a small step change in the turbine control valve position in the opposite direction. The ITC was calculated iteratively using the resultant power and temperature changes along with an assumed power coefficient. The moderator temperature coefficient (MTC) was then calculated by subtracting the predicted fuel temperature coefficient (FTC) from the measured isothermal temperature coefficient (ITC).

4.5.3 Results and Evaluation

Acceptance criteria state the following:

- a. The measured ITC shall agree with the predicted values within $\pm 0.3 \times 10^{-4} \Delta k/k/^{\circ}F$;
- b. The measured power coefficient should agree with the predicted values within $\pm 0.3 \times 10^{-4} \Delta k/k/\%$ power; and
- c. The MTC shall be less positive than $+ 0.5 \times 10^{-4} \Delta k/k/^{\circ}F$ when reactor power is $\leq 70\%$ of rated thermal power and less positive than 0.0 when reactor power is $> 70\%$ of rated thermal power and less negative than $- 2.8 \times 10^{-4} \Delta k/k/^{\circ}F$ at rated thermal power.

These criteria were met at both the 50% and 100% test plateaus. Table 4.5-1 tabulates the results of the reactivity coefficient measurements at 50% and 100% full power.

TABLE 4.5-1
REACTIVITY COEFFICIENTS AT
50% AND 100% FULL POWER

TEST PLATEAU	PARAMETER	WITH CENTER CEA MOVEMENT		WITHOUT CENTER CEA MOVEMENT	
		PREDICTED	MEASURED	PREDICTED	MEASURED
50% Full Power	ITC ($\Delta\rho/^{\circ}\text{F}$)	$-.57 \times 10^{-4}$	$-.31 \times 10^{-4}$	N/A	N/A
	PC ($\Delta\rho/\% \text{ Power}$)	$-.94 \times 10^{-4}$	-1.07×10^{-4}	N/A	N/A
	MTC ($\Delta\rho/^{\circ}\text{F}$)	$-.43 \times 10^{-4}$	$-.17 \times 10^{-4}$	N/A	N/A
100% Full Power	ITC ($\Delta\rho/^{\circ}\text{F}$)	N/A	N/A	-1.11×10^{-4}	$-.96 \times 10^{-4}$
	PC ($\Delta\rho/\% \text{ Power}$)	N/A	N/A	$-.81 \times 10^{-4}$	N/A
	MTC ($\Delta\rho/^{\circ}\text{F}$)	N/A	N/A	$-.98 \times 10^{-4}$	$-.83 \times 10^{-4}$

5.0 CONCLUSION

The results of the Arkansas Nuclear One Unit 2 Cycle 3 reload test program summarized in the body of this report:

- (1) Verify that the core was correctly loaded with regard to the utilized fuel management plan and that there are no detectable anomalies present which would result in unsafe operation of the plant during the length of the cycle.
- (2) Computational models utilized in designing the reload core and performing the safety analysis for Cycle 3 adequately predict core behavior during this cycle.

The ANO-2 Cycle 3 reload core was demonstrated to be properly designed, fabricated and installed. The unit can be operated in a manner that should not pose undue risk to the health and safety of the public.